Predicting Plaque Area Increase and Plaque Burden Increase Using Patient-Specific Fluid-Structure-Interaction Models Based on IVUS and OCT Images with Follow-Up

†Xiaoya Guo,[1] Dalin Tang,[1*,2] David Molony,[3] Chun Yang,[2] Habib Samady[3], Jie Zheng[4], Gary S. Mintz[5], Akiko Maehara[5], Jian Zhu[6], Genshan Ma[6], Don P. Giddens[3,7]

[1] Department of Mathematics, Southeast University, Nanjing, 210096, China
[2] Mathematical Sciences Department, Worcester Polytechnic Institute, Worcester, MA 01609 USA
[3] Department of Medicine, Emory University School of Medicine, Atlanta, GA, 30307, USA
[4] Mallinckrodt Institute of Radiology, Washington University, St. Louis, MO, 63110, USA
[5] The Cardiovascular Research Foundation, Columbia University, New York, NY 10022, USA
[6] Department of Cardiology, Zhongda Hospital, Southeast University, Nanjing, 210009, China
[7] The Wallace H. Coulter Department of Biomedical Engineering,
Georgia Institute of Technology, Atlanta, GA, 30332 USA

† Presenting author: Xiaoya Guo, Southeast University, Nanjing China;
* Corresponding authors: Dalin Tang, Southeast University, Nanjing China, email: dtang@wpi.edu, fax number: 508 831-5824;

Abstract

Atherosclerotic plaque progression may be associated with morphological and mechanical factors. Plaque morphological information on IVUS and OCT images could complement each other and provide for more accurate plaque morphology. Fluid-structure interaction (FSI) models combining intravascular ultrasound (IVUS) and optical coherence tomography (OCT) were constructed to obtain mechanical risk factors. Accuracy and completeness of imaging and advanced modeling lead to accurate plaque progression predictions.

In vivo IVUS and OCT coronary plaque data at baseline and follow-up were acquired from left circumflex coronary and right coronary artery of one patient. Co-registration and segmentation of baseline and follow-up IVUS and OCT images were performed by experts. Baseline and follow-up 3D FSI models based on IVUS and OCT were constructed to obtain plaque stress, strain and flow shear stress for plaque progression prediction. Nine factors including 6 morphological factors and 3 mechanical factors were selected for each slice. Plaque area increase (PAI) and plaque burden increase (PBI) were chosen to measure plaque progression. All possible combinations of nine factors were fed to a generalized linear mixed model for PAI and PBI prediction and quantification of their prediction accuracies.

Prediction accuracy is defined as the sum of sensitivity and specificity. The optimized predictor combining 9 factors gave the best prediction for PAI with accuracy=1.7087 (sensitivity: 0.8679; specificity: 0.8408). Plaque wall strain (PWSn) was the best single-factor predictor for PAI with accuracy=1.5918 (sensitivity: 0.7143; specificity 0.8776). A combination of average cap thickness, calcification area, plaque area, plaque wall stress and plaque wall strain gave the best prediction for PBI with accuracy=1.8698 (sensitivity: 0.8892; specificity: 0.9806). PWSn was the best single-factor predictor with accuracy=1.8461 (sensitivity: 0.8784; specificity 0.9677).

Combining morphological and mechanical risk factors may lead to more accurate progression prediction, compared to the predictions using single factors. IVUS+OCT formed basis for accurate data for morphological and mechanical factors.

Keywords: Vulnerable plaque; OCT; IVUS; plaque progression; patient-specific FSI model.

1. Introduction

Atherosclerotic plaque progression and rupture may be associated with complicated factors including plaque morphology, material properties, mechanical factors, cell and genomic activities, etc. [1-2]. In original study for plaque progression, research groups performed large-scale studies based on histologic sections from autopsy to investigate plaque remodeling and vulnerability [3-5]. For in vivo studies, Mintz et al., Nakamura et al. and among others used medical imaging such as intravascular ultrasound (IVUS) and angiography and indicated that plaque area and lumen cross-sectional area were closely related to plaque progression [6-8]. The limitation of these earlier research is that it only gave one-time plaque data and did not reflect plaque progression. Follow-up studies with advanced medical images can better track the plaque progression. Several research groups used plaque area and plaque burden as the measurement of plaque progression respectively, and investigated the correlation between plaque progression and wall shear stress (WSS) from follow-up data [9-11]. Plaque progression is influenced by the interaction of various morphological factors and mechanical factors including structural and flow conditions, and its mechanism has not been fully understood [2,12]. Wang et al. used fluid-structure interaction (FSI) models with follow-up VH-IVUS data and showed that the combination of morphological and biomechanical factors could improve prediction accuracy, compared to predictions using only morphological features [13].

In recent years, Optical Coherence Tomography (OCT) with high resolution (15-20 μm) gradually became a powerful tool in identifying thin fibrous cap (cap thickness < 65 μm), inflammation and calcification [14-16]. Uemura et al. used 7-month follow-up OCT data from 53 patients to study the relation between morphological characteristics and plaque progression, and found a high correlation between thin-cap fibroatheroma and subsequent luminal progression [17]. One limitation of OCT is its limited penetration: OCT cannot "see" through the whole vessel wall. Plaque morphological information on IVUS and OCT images could complement each other and provide more complete and accurate plaque morphology, especially more accurate fibrous cap thickness measurements [18]. Since accurate cap thickness and stress/strain quantifications are of fundamental importance for vulnerable plaque research, Guo et al. proposed a modeling method to combine IVUS and OCT for more accurate patient-specific coronary morphology and stress/strain calculations [19]. This IVUS+OCT-based modeling approach may provide the basis leading to better plaque stress/strain calculations and progression and vulnerability predictions.

In this paper, patient follow-up IVUS and OCT data were acquired and FSI models were constructed to better quantify human coronary atherosclerotic plaque morphology (especially cap thickness) and plaque stress/strain conditions. Nine selected plaque morphological and mechanical factors and all possible combination were used into generalized linear mixed models (GLMM) to predict plaque progression measured by plaque area increase (PAI) and plaque burden increase (PBI).

2. Data, Models and Methods

2.1 IVUS and OCT data acquisition and image processing

Baseline and one-time follow-up in vivo IVUS/OCT/Angiography data were acquired from two arteries (left circumflex coronary artery and right coronary artery) of one participant (female, 80 age) at Emory University with informed content obtained. IVUS catheterization (Boston Scientific/SCIMED Corp.) was performed with an automatic pullback speed of 0.5mm/s. Following IVUS image acquisition, OCT catheterization (St. Jude, Minnesota, MN) was also performed with an automatic pullback speed of 20mm/s. The IVUS/OCT/Angiography data at baseline (Time 1, T1) and follow-up (Time 2, T2) were acquired uniformly according to the above descriptions. As IVUS and OCT images at T1 and T2 were recorded using different

catheter in four pullbacks, they must be registered both longitudinally and circumferentially in order to be used for modeling. Co-registration and segmentation of paired IVUS and OCT were performed by experts. Paired IVUS and OCT were merged to obtained IVUS+OCT slices, with IVUS providing whole vessel (lumen and out-boundary) contours, and OCT provide more accurate cap thickness and plaque component contours. All image slices were segmented into 3 plaque tissue types: Fibrotic plus Fibro-fatty, Necrotic core, and Dense Calcium.

2.2 The 3D FSI model and Mooney-Rivlin model for material properties

Aortic pressure (136/88 mmHg) obtained by catheter were used as inlet pressure conditions. The modeling procedures, assumptions, governing equations and boundary conditions for the 3D FSI model can be found in our previous publication [20]. Atherosclerotic vessels were stiffer than healthy vessels, axial shrinkage was set at 5% in our models. The anisotropic Mooney-Rivlin model was used for the vessel tissue. Its strain energy density function is:

$$W=c_1(I_1-3)+c_2(I_2-3)+D_1[\exp(D_2(I_1-3))-1]+(K_1/K_2)\{\exp[K_2(I_4-1)^2]-1\}, \quad (1)$$

$$I_1=\sum C_{ii},\ I_2=\tfrac{1}{2}[I_1^2-C_{ij}C_{ij}], \quad (2)$$

where I_1 and I_2 are the first and second invariants of right Cauchy-Green deformation tensor $\mathbf{C}$ defined as $\boldsymbol{C}=[C_{ij}]=\mathbf{X}^T\mathbf{X}$, $\mathbf{X}=[X_{ij}]=[\partial x_i/\partial a_j]$, (x_i) is current position, (a_i) is original position, $I_4=C_{ij}(\mathbf{n}_c)_i(\mathbf{n}_c)_j$, $\mathbf{n}_c$ is the unit vector in the circumferential direction of the vessel, c_1, c_2, D_1, D_2, K_1 and K_2 are material parameters [20,21] whose values were determined using in vivo IVUS data [22]: c_1=-262.6 kPa, c_2=22.9, D_1=125.9 kPa, D_2=2, K_1=7.19 kPa, K_2=23.5.

Plaque components were assumed isotropic and the isotropic Mooney-Rivlin material model was used to describe their material properties.

$$W_{iso}=c_1(I_1-3)+c_2(I_2-3)+D_1[\exp(D_2(I_1-3))-1], \quad (3)$$

The material parameters: Lipid: c_1=0.5 kPa, c_2=0, D_1=0.5 kPa, D_2=1.5. Calcification: c_1=92 kPa, c_2=0, D_1=36 kPa and D_2=2 [22]. The models were solved by a commercial finite element software ADINA (Adina R & D, Watertown, MA, USA) following established procedures [20].

2.3 Data Extraction and Plaque Measurements

The contours segmented from IVUS+OCT slices were used to make FSI models and obtain morphological and mechanical measurements for analysis. Each slice contained 100 evenly-spaced nodal points taken on the lumen, each lumen nodal point was connected to a corresponding point on vessel out-boundary. If the connecting line pass through lipid region, the distance between lumen nodal point and first time the line meets the lipid is defined cap thickness. The average of cap thickness from one slice was defined as average cap thickness (Ave. CT). The area of lipid or calcification (denoted as Ca) in slice was recorded as lipid or Ca area. The area in lumen contour was denoted lumen area (LA). The area between lumen and out-boundary was defined as plaque area (PA). The plaque burden (PB) was defined as the ratio of PA to the sum of PA and LA. Plaque wall stress (PWS) and plaque wall strain (PWSn), WSS were extracted from 3D FSI model solution at 100 lumen nodal points of all slices. Therefor, morphological and mechanical factors uesd in this study included Ave. CT, lipid/Ca area, LA, PA and PB. WSS, PWS and PWSn.

2.4 Plaque Progression Classification and Prediction

For all paired slices, plaque area increase (PAI) and plaque burden increase (PBI) from T1 to T2 were selected to measure plaque progression:

Plaque Area Increase (PAI) = (PA at T2) - (PA at T1). (4)

Plaque Burden Increase (PBI) = (PB at T2) - (PB at T1). (5)

In this work, plaque progression was classified into two types in this work. For a given slice, if PAI > 0, then this slice was labeled 1. If PAI ≤ 0, this slice was labeled -1. Slice labeling for PBI was done in the same way as PAI. Generalized linear mixed models (GLMM) were used

to calculate the predictive sensitivity and specificity of all possible combinations of the 9 risk factors (predictors) and find the best combination for plaque progression prediction. Details about GLMM can be found in [23]. A five-fold cross-validation procedure was employed in all 105 slices from two arteries for training and testing sets. For the reliability of results, 100 times repeated experiment were performed. Prediction accuracy is defined as the sum of sensitivity and specificity (Sen+Spe). The receiver operating characteristic curve (ROC) and the area under of the ROC curve were also given to compare the prediction accuracy.

3. Results

3.1 Plaque progression prediction using one single risk factor

For the nine morphological and mechanical factors, each factor was tested to find the best single risk factor for plaque progression prediction. Prediction results from different single factor and plaque progression measurement were compared. According to the sum of sensitivity and specificity, the best five single risk factors for PAI and PBI are showed in Table 1. PWSn was the best predictor for both PAI and PBI. The sum of sensitivity and specificity are 1.5918 and 1.8461 respectively. The ROC curves of PWSn using PAI and PBI were shown in Figure 1. The AUC values were 0.8126 and 0.9529, respectively.

Table 1. Prediction sensitivity and specificity using one single factor using PAI and PBI.

	Predictors	ProbCutoffs	Sensitivity	Specificity	Sen+Spe	AUC
PAI	PWSn	0.5110	0.7143	0.8776	1.5918	0.8126
	PWS	0.5042	0.6679	0.7592	1.4270	0.7477
	Ca Area	0.4988	0.4964	0.9184	1.4148	0.6874
	Ave. CT	0.4606	0.5786	0.7306	1.3092	0.6379
	LA	0.4974	0.5679	0.6939	1.2617	0.6336
PBI	PWSn	0.8304	0.8784	0.9677	1.8461	0.9529
	LA	0.8049	0.6432	0.9935	1.6368	0.8022
	Lipid Area	0.6345	0.7108	0.9032	1.6140	0.8168
	PB	0.7487	0.6838	0.9032	1.5870	0.7606
	FSS	0.7656	0.6811	0.9032	1.5843	0.7840

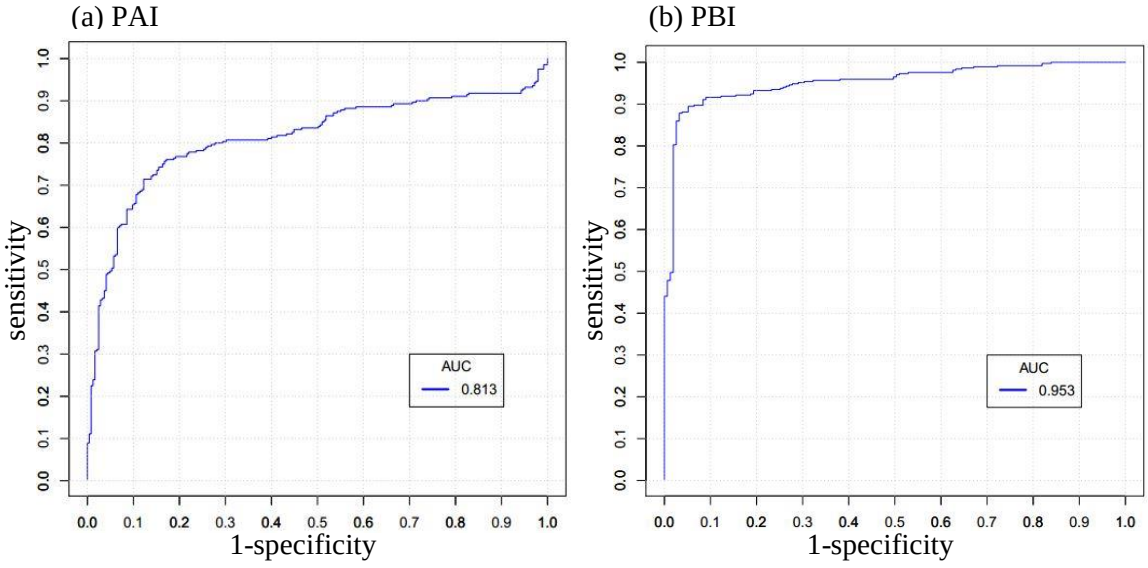

Figure 1. ROC curve and AUC value using PWSn to predict PAI and PBI.

3.2 Plaque progression prediction using combination of risk factors

Table 2 gives two best combinations of nine eight risk factors with PAI and PBI. Using PAI as the measure of plaque progression, the combination of Lipid area, Ave. CT, Ca area, LA, PA, PB, PWS, PWSn, and FSS showed the best prediction accuracy (Sen+Spe: 1.7087). Using PBI as the measure of plaque progression, the combination of Ave. CT, Ca area, PA, PWS, and PWSn gave the best prediction accuracy (Sen+Spe: 1.8698). The ROC curves of best combination using PAI and PBI were shown in Figure 2. The AUC values of best combination were 0.8632 and 0.9584, respectively.

Table 2. Prediction sensitivity and specificity using one single factor using PAI and PBI.

	Predictors	ProbCutoffs	Sensitivity	Specificity	Sen+Spe	AUC
PAI	Lipid Area+Ave. CT +Ca Area+LA+PA+PB +PWS+PWSn+FSS	0.3051	0.8679	0.8408	1.7087	0.8632
	Lipid Area+Ca Area +PA+PB+PWSn	0.3941	0.8857	0.8082	1.6939	0.9215
PBI	Ave. CT+Ca Area+PA +PWS+PWSn	0.8629	0.8892	0.9806	1.8698	0.9584
	Ave. CT+CaArea +PWSn+FSS	0.8373	0.8784	0.9871	1.8655	0.9522

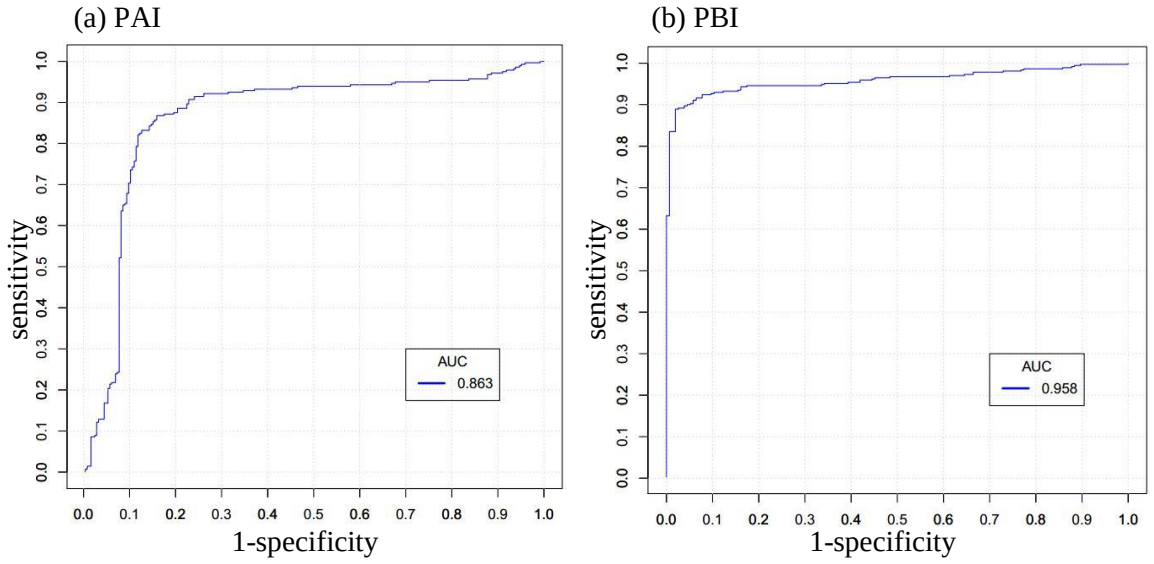

Figure 2. ROC curve and AUC value using best combination of factors to predict PAI and PBI.

4. Discussion

4.1 Significance of combining OCT and IVUS.

The accurate plaque progression prediction depends on accurate simulation, while accurate model depends on high resolution of medical imaging. Imaging resolution has been a major limitation for vulnerable plaque research since the introduction of medical imaging. The resolution for IVUS (100-150 μm) or MRI (300 μm) which is not enough to identify vulnerable

plaques with thin cap thickness < 65 micron. The combination of OCT and IVUS could possess the capabilities of detecting thin fibrous cap and penetrating vessel thickness. OCT+IVUS is able to provide more accurate cap thickness information to promote both the morphological and mechanical analyses in vulnerable plaque research.

4.2 Significance of combining mechanical and morphological risk factors for plaque progression prediction.

Most plaque progression research group paid attention to morphological factors and flow shear stress and seldom considered structural plaque stress and strain [9,10]. While it is well accepted that mechanical forces play an important role in plaque progression, research work based on patient follow-up data demonstrating that is rare. In fact, plaque mechanical state is affected by both fluid and structure forces. Tang's group used FSI models and patient follow-up data to investigate the influence of structural stress/strain for plaque vulnerability and progression [2]. By using OCT and IVUS data with follow-up, we constructed coronary plaque FSI models with cycle bending and perform progression prediction using nine morphological and mechanical risk factors. Our pilot study indicated that combining morphological and mechanical factors could give better predictions.

4.3 Limitations

One major limitation of this study is lack of histology data as the golden standard. Manual segmentation results based on IVUS and OCT images were considered as the alternative to the golden standard. Another limitation is the small sample size of OCT image studied. Large-scale studies with more OCT image are needed to validate and improve the significance of prediction method.

5. Conclusion.

Combining morphological and mechanical risk factors may lead to more accurate progression prediction, compared to the predictions using single factors. IVUS+OCT formed basis for accurate data for morphological and mechanical factors.

Funding:

This research was supported in part by NIH grant R01 EB004759 and a Jiangsu Province Science and Technology Agency grant BE2016785.

There are no conflicts of interest in this study.

References

1. Friedman MH, Krams R, Chandran KB. Flow interactions with cells and tissues: cardiovascular flows and fluid-structure interactions. *Annals Biomedical Engineering* 2010;38(3):1178-1187.
2. Tang D, Kamm RD, Yang C, Zheng J, Canton G, Bach R, Huang X, Hatsukami TS, Zhu J, Ma G, Maehara A. Image-based modeling for better understanding and assessment of atherosclerotic plaque progression and vulnerability: Data, modeling, validation, uncertainty and predictions. *Journal of Biomechanics* 2014; 47(4):834-846.
3. Clarkson TB, Prichard RW, Morgan TM, Petrick GS, Klein KP. Remodeling of coronary arteries in human and nonhuman primates. *JAMA* 1994;271: 289-294.
4. Glagov S, Weisenberg E, Zarins CK, Stankunavicius R, Kolettis GJ. Compensatory enlargement of human atherosclerotic coronary arteries. *N Engl J Med* 1987;316:1371–1375.
5. Zarins CK, Weisenberg E, Kolettis G, Stankunavicius R, Glagov S. Differential enlargement of artery segments in response to enlarging atherosclerotic plaques. *J Vasc Surg*. 1988;7:386–394.
6. Gerber TC, Erbel R, Gorge G, Ge J, Rupprecht H-J, Meyer J. Extent of atherosclerosis and remodeling of the left main coronary artery determined by intravascular ultrasound. *Am J Cardiol* 1994;73:666–671.

7. Mintz GS, Kent KM, Pichard AD, Satler LF, Popma JJ, Leon MB. Contribution of inadequate arterial remodeling to the development of focal coronary artery stenosis. An intravascular ultrasound study. *Circulation* 1997;95:1791–1798.
8. Nakamura Y, Takemori H, Shiraishi K, et al. Compensatory enlargement of angiographically normal coronary segments in patients with coronary artery disease: in vivo documentation using intravascular ultrasound. *Angiology* 1996;47:775–781.
9. Stone GW, Maehara A, Lansky AJ, de Bruyne B, Cristea E, Mintz GS, Mehran R, McPherson J, Farhat N, Marso SP, Parise H, Templin B, White R, Zhang Z, Serruys PW. The PROSPECT Investigators: A prospective natural-history study of coronary atherosclerosis. *N. Engl. J. Med*. 2011;364 (3):226–235.
10. Samady H, Eshtehardi P, McDaniel MC, Suo J, Dhawan SS, Maynard C, Timmins LH, Quyyumi AA, Giddens DP, Coronary artery wall shear stress is associated with progression and transformation of atherosclerotic plaque and arterial remodeling in patients with coronary artery disease. *Circulation* 2011;124, 779–788.
11. Corban MT, Eshtehardi P, Suo J, McDaniel MC, Timmins LH, RassoulArzrumly E, Maynard C, Mekonnen G, King 3rd S, Quyyumi AA, Giddens DP, Samady H. Cobination of plaque burden, wall shear stress, and plaque phenotype has incremental value for prediction of coronary atherosclerotic plaque progression and vulnerability. *Atherosclerosis* 2014;232, 271–276.
12. Maurice RL, Ohayon J, Finet G, Cloutier G. Adapting the Lagrangian speckle model estimator for endovascular elastography: theory and validation with simulated radio-frequency data. *J. Acoust. Soc. Am*. 2004;116 (2), 1276–1286.
13. Wang L, Tang D, Maehara A, Wu Z, Yang C, Muccigrosso D, Zheng J, Bach R, Billiar KL, Mintz GS. Fluid-structure interaction models based on patient-specific IVUS at baseline and follow-up for prediction of coronary plaque progression by morphological and biomechanical factors: A preliminary study. *Journal of biomechanics.* 2018;68:43-50.
14. Tearney GJ, Regar E, Akasaka T, Adriaenssens T, Barlis P, Bezerra HG, Bouma B, Bruining N, Cho JM, Chowdhary S, Costa MA. Consensus standards for acquisition, measurement, and reporting of intravascular optical coherence tomography studies: a report from the International Working Group for Intravascular Optical Coherence Tomography Standardization and Validation. *Journal of the American College of Cardiology*. 2012;59(12):1058-72.
15. Burke AP, Kolodgie FD, Farb A, Weber D, Virmani R. Morphological predictors of arterial remodeling in coronary atherosclerosis. *Circulation.* 2002;105(3):297-303.
16. Brown AJ, Obaid DR, Costopoulos C, Parker RA, Calvert PA, Teng Z, Hoole SP, West NE, Goddard M, Bennett MR. Direct comparison of virtual-histology intravascular ultrasound and optical coherence tomography imaging for identification of thin-cap fibroatheroma. *Circ. Cardiovasc Imaging*. 2015;8(10): e003487.
17. Uemura S, Ishigami KI, Soeda T, Okayama S, Sung JH, Nakagawa H, Somekawa S, Takeda Y, Kawata H, Horii M, Saito Y. Thin-cap fibroatheroma and microchannel findings in optical coherence tomography correlate with subsequent progression of coronary atheromatous plaques. *European heart journal.* 2011;33(1):78-85
18. Räber L, Heo JH, Radu MD, Garcia-Garcia HM, Stefanini GG, Moschovitis A, Dijkstra J, Kelbaek H, Windecker S, Serruys PW. Offline fusion of co-registered intravascular ultrasound and frequency domain optical coherence tomography images for the analysis of human atherosclerotic plaques. *EuroIntervention.* 2012;8(1):98-108.
19. Guo X, Giddens DP, Molony D, Yang C, Samady H, Zheng J, Mintz GS, Maehara A, Wang L, Pei X, Li ZY. Combining IVUS and Optical Coherence Tomography for More Accurate Coronary Cap Thickness Quantification and Stress/Strain Calculations: A Patient-Specific Three-Dimensional Fluid-Structure Interaction Modeling Approach. *Journal of biomechanical engineering*. 2018;140(4):041005
20. Yang C, Bach R, Zheng J, Naqa IE, Woodard PK, Teng Z, Billiar KL, Tang D. "*In vivo* IVUS-Based 3D Fluid Structure Interaction Models with Cyclic Bending and Anisotropic Vessel Properties for Human Atherosclerotic Coronary Plaque Mechanical Analysis," *IEEE Trans. Biomed. Engineering,* 2009;56(10): 2420-2428
21. Holzapfel GA, Nonlinear Solid Mechanics: A Continuum Approach for Engineering, Wiley, Chichester, 2000; New York
22. Guo X, Zhu J, Maehara A, Monoly D, Samady H, Wang L, Billiar KL, Zheng J, Yang C, Mintz GS, Giddens DP. Quantify patient-specific coronary material property and its impact on stress/strain calculations using in vivo IVUS data and 3D FSI models: a pilot study. *Biomechanics and modeling in mechanobiology*. 2017;16(1):333-44
23. Wu Z, Yang C, Tang D. In vivo serial MRI-based models and statistical methods to quantify sensitivity and specificity of mechanical predictors for carotid plaque rupture: location and beyond. *Journal of biomechanical engineering.* 2011;133(6):064503.